Lean female mice producing *trans* 10, *cis* 12-conjugated linoleic acid present excessive fibroblast growth factor 21, adrenaline, prostaglandin E2, corticosterone, and glucagon

Yu Rao[1,2,#], Lu-Wen Liang[1,#], Mei-Juan Li[3,#], Yang-Yang Wang[1], Bao-Zhu Wang[1], Ke-Mian Gou[1,2,*]

[1]*Institute of Comparative Medicine,* [2]*Jiangsu Co-innovation Center for Prevention and Control of Important Animal Infectious Diseases and Zoonoses, Department of Experimental Zoology, College of Veterinary Medicine, Yangzhou University, Yangzhou 225009, China*;

[3]*Institute of Animal Husbandry and Veterinary Science, Guizhou Academy of Agricultural Sciences, Guiyang 550005, China.*

# These authors contributed equally to this work.

*Corresponding author: Kemian Gou, College of Veterinary Medicine, Yangzhou University, Wenhui South Road, Yangzhou 225009, China.

Email: gou@yzu.edu.cn

ABSTRACT

Dietary *trans* 10, *cis* 12-conjugated linoleic acid (t10c12-CLA) has been shown to induce white fat reduction. In this study, the transgenic mice that produce endogenous t10c12-CLA were used to determine the long-term impact of this substance on lipid metabolism in lean female mammals. Phenotype profiling showed that the t10c12-CLA did not induce fat loss but resulted in less heat release and oxygen consumption, as well as excessive adrenaline, tumour necrosis factor-alpha, and interleukin-6 in either biallelic Pai/Pai or monoallelic Pai/wt mice compared to their wild-type littermates. Furthermore, the following effects of t10c12-CLA were genotype-specific. Pai/wt mice specifically exhibited increased chronic fibroblast growth factor 21 (FGF21) and reduced physical activities. Contrarily, Pai/Pai mice showed the overproduction of prostaglandin E2 (PGE2), corticosterone, and glucagon, accompanied by hypertriglyceridemia and fatty liver. Further analysis of Pai/Pai livers revealed that the steatosis resulted from attenuated lipid metabolism via down-regulating phosphorylated AMP-activated protein kinase (AMPK) and fatty acid synthase. Analysis of Pai/Pai brown adipose tissue indicated stimulated thermogenesis and lipolysis by up-regulating uncoupling proteins 1 and 2, phosphorylated hormone-sensitive lipase, carnitine palmitoyltransferase 1B, and AMPK, as well as down-regulating phosphorylated AMPK. These results suggest that chronic t10c12-CLA may affect lipid metabolism by stimulating the overproduction of multiple hormones (FGF21, PEG2, adrenaline, etc.) in a dose-dependent manner in lean female mammals. It also suggests that t10c12-CLA-induced fatty liver, inflammation, hypothermia and excess hormones are major health concerns.

Keywords: conjugated linoleic acid; prostaglandin E2; steatosis; adrenaline; inflammation; brown adipose tissue

43 **1. INTRODUCTION**

44

45 *Trans* 10, *cis* 12-conjugated linoleic acid (t10c12-CLA) occurs naturally in small
46 amounts in foods such as beef and dairy products. Its popular health benefit is reducing body
47 fat by increasing energy expenditure via browning of white adipose tissue (WAT) [1,2] or
48 uncoupling protein (UCP) 1 & 2-mediated thermogenesis in brown adipose tissue (BAT) [3],
49 promoting biosynthesis of N-lactoyl-phenylalanine via the up-regulation of cytosolic
50 nonspecific dipeptidase 2 in WAT [4], or increasing intramuscular fat [5]. In addition, it has
51 other potential health influences, including protecting against atherosclerosis by modulating
52 the macrophage phenotype [6], promoting beneficial effects on cholesterol efflux [7], reducing
53 oxidative stress [8], changing intestinal microbiota [9] and metabolite profiles [5], even down-
54 regulating Alzheimer's hallmarks in an aluminium mouse through an Nrf2-mediated
55 adaptive response and increasing brain glucose transporter levels [10].

56 Although the potential health benefits, especially the fat loss properties of dietary
57 t10c12-CLA, have been extensively studied in obese animals, the potential health benefits in
58 lean animals have not been clarified fully. A study in lean male mice treated with dietary
59 t10c12-CLA observed a dramatic reduction in fat mass in the first two weeks which
60 interestingly rebounded during the following 3-5 weeks due to a massive accumulation of
61 lipids in the liver [11]. At the same time, other studies have confirmed its fat loss properties
62 but indicated its side effects result in fatty liver in male [9,11] or female lean mice [12-16].

63 In our previous study, we produced a transgenic mouse that can produce t10c12-
64 CLA after inserting the foreign gene encoding the *Propionibacterium acnes* isomerase (PAI)
65 into the Rosa26 locus [3]. This Rosa26-Pai knock-in mouse exhibited continuous production
66 of t10c12-CLA and can be used to elucidate its enduring influence on overall health. In its
67 lean male offspring, fat reduction in biallelic Pai/Pai, not in monoallelic Pai/wt genotypes
68 suggests t10c12-CLA's impact is dose-dependent. Additionally, low doses of t10c12-CLA
69 possibly play an active role in lipid metabolism by stimulating the fibroblast growth factor
70 21 (FGF21) secretion. Whereas the high doses of t10c12-CLA possibly induce fat reduction
71 by promoting energy expenditure via UCP1/2-mediated BAT thermogenesis [3].

72 The current study continued to investigate the adiposity characteristics and
73 metabolic profiles of these lean female mice. In contrast to their male counterparts, the
74 findings of this study demonstrate that Pai female mice did not experience changes in body
75 fat but did experience a decrease in heat release. Moreover, specific metabolic features in

76 Pai/wt female mice have confirmed that the low doses of t10c12-CLA can induce the
77 overproduction of FGF21, while the high doses of t10c12-CLA stimulate excessive
78 prostaglandin E2 (PGE2), corticosterone, and glucagon which probably affect the lipid
79 metabolism via varies of pathways. The results suggest that Pai mice may be a useful model
80 to investigate the chronic t10c12-CLA's effects and its mechanisms of action in the body. It
81 also indicates that t10c12-CLA-induced fatty liver, inflammation, hypothermia and excess
82 hormones are major health concerns.

2. MATERIALS AND METHODS

2. 1. Mice and diet

The transgenic founder from a hybrid embryo of DBA/2 and C57BL/6J was backcrossed to C57BL/6J mice for more than eight generations, and then the monoallelic Pai/wt matings were used to produce the Pai/Pai, Pai/wt, and wild-type (wt) offspring for this study. Genotyping was performed using genomic DNA from tail tissues, with the presence of the Pai gene being assayed by amplifying the 514-bp Pai fragments (forward: 5-taaccatgttcatgccttcttc-3; reverse: 5-caccttgttgtagtgtccgttt-3) and the wt Rosa26 sequence being assayed by amplifying the 605-bp fragments that spanned the insertional site of the Rosa26 locus (forward: 5-ccaaagtcgctctgagttgttatcagt-3; reverse: 5-ggagcgggagaaatggatatgaag-3). PCR amplification was performed for 30 cycles at 94°C for 30 sec, 57°C for 30 sec, and 72°C for 40 sec.

Table 1. Sources of dietary ingredients

Ingredients	Grams	Sources
Lactic casein	200.0	Gansu Hualing Dairy Co. Ltd, Hezuo city, China
L-cystine	3.0	Zhongtuan shihua Food Reagents Co. Ltd, Hangzhou, China
Sucrose	176.8	Jinhuitaiya, Chemcal Reagents Co. Ltd, Tianjin, China
Corn Starch	452.2	Zhucheng Xingmao Corn Co. Ltd, Weifang city, China
Maltodextrin 10	75.0	Dongzhu Food Co. Ltd, Guilin city, China
Cellulose	50.0	Yisheng Kangyuan Biotech Co. Ltd, Zibo city, China
Soybean oil	25.0	Shandong Luhua Co. Ltd, Leiyang, China
Lard	20.0	Yaodong Baofengyuan Co. Ltd, Qingdao, China
Mineral Mix (20x)	50.0	Mingxin Chemical Reagents Co. Ltd, Zhenzhou, China
Choline bitartrate	2.0	Zhejiang Linuo Biotech Co. Ltd, Yiwu, China
Vitamin Mix (1000x)	1.0	Mingxin Chemical Reagents Co. Ltd, Zhenzhou, China
Total Gram	1055	

Mice of the above three genotypes aged 11-15 weeks were used for analysis in this study unless otherwise specified. All animal experiments were conducted in accordance with the guidance provided by the Committee for Experimental Animals of Yangzhou University. The animal study protocol was approved by the Ethics Committee of Yangzhou University (protocol code NSFC2020-SYXY-20 and dated 25 March 2020). The mice were housed in a

light-controlled room (12L:12D, lights on at 0700 h) at a temperature of 22-23°C and fed ad libitum with a standard diet containing 10% kcal% fat. Fresh diets were prepared every month in accordance with formula No. D12450H of OpenSource DIETS™ (Research Diets Inc., NJ, USA) under sterile conditions. The composition of the D12450H and the sources of the food-grade ingredients used in the diets are provided in Table 1.

2. 2. Major methods

The procedures utilised in this study, including gas chromatography, real-time RNA and proteins analyses, histological analysis, intraperitoneal glucose (2g/kg body weight) and insulin (0.5 IU/kg body weight) tolerance tests, hepatic and blood parameter measurements, and experiments conducted in metabolic cages, were performed following the standard methods as described in our previous study of transgenic male mice [3].

2.3. Measurement of serum estradiol

Three-week-old mice were injected intraperitoneally with 5 IU pregnant mare serum gonadotrophin (Jinmu Biotech Co. Ltd., Wuxi, China), and 48 h later, blood was collected from the orbital vein of anaesthetised mice and used to measure the serum estradiol levels using the E2 ELISA kit (Meimian Industrial Co. Ltd., Jiangsu, China).

2. 4. Statistical analysis.

Analysis was conducted using GraphPad Prism 8.0 (GraphPad Software Inc.; La Jolla, CA, USA). Comparisons between wt and Pai/Pai samples were performed using an unpaired two-tailed t-test with Welch's correction where appropriate. Multiple comparisons among wt, Pai/wt, and Pai/Pai groups were performed using one-way ANOVA and Brown-Forsythe and Welch tests. Data are presented as mean ± standard deviation (SD), and $p < 0.05$ was considered statistically significant.

3. RESULTS

3. 1. Fatty acids analysis

Gas chromatography was used to analyse the compositions of fatty acids (FAs) in the livers, kidneys, hearts, tibialis anterior muscle, and interscapular BAT. The content of t10c12-CLA had increased by 69% in the Pai/wt kidneys compared to wt littermates ($p < 0.05$; Table 2). However, the quantities of substrate linoleic acid had decreased in the Pai/Pai livers by 23% and skeletal muscle by 34% and had increased by 36% in the Pai/wt kidneys ($p < 0.05$; Supplementary Table 1).

The contents of other FAs such as myristic (14:0), palmitic (16:0), stearic (18:0), palmitoleic (16:1n-7), cis-vaccenic (18:1n-7), oleic (18:1n-9), arachidonic (20:4n-6), and docosahexaenoic (22:6n-3) acids were changed to varying degrees in one or more tissues (Supplementary Table 1), This suggests that the changes in the content of each FA were genotype- or tissue-specific. Additionally, the amounts of total FAs (mg/g) increased in the Pai/wt kidneys (10.2 ± 1.39 versus 13.3 ± 1.69; $p < 0.05$), similar to our previous study in Pai/wt male mice [3]. These results suggest lipopathy in the Pai/wt kidney.

Table 2. Content comparison of t10c12-CLA (μg/g) in wild-type and Pai mice

	wild-type (n)	Pai/wt (n)	Pai/Pai (n)
Liver	2.56 ± 3.24 (7)	4.30 ± 4.10 (5)	ND (5)
Kidney	6.50 ± 1.25[a] (5)	11.0 ± 3.65[b] (6)	6.09 ± 0.42[a] (4)
Heart	ND (5)	ND (4)	ND (4)
Muscle	ND (4)	ND (4)	ND (4)
Brown adipose tissue	22.4 ± 15.9 (4)	29.5 ± 7.5 (4)	29.8 ± 0.5 (4)

Note: Tissues from 11-week-old mice was analysed by gas chromatography and 19:0 is an internal standard. ND, not detected. Each value represents the mean ± SD and the numbers in brackets indicate the size of the tested samples. Different letters in superscript indicate a level of statistical significance of $p < 0.05$.

3. 2. Growth analysis

There was a significant difference in weaning weight among the three genotypes (wt > Pai/wt > Pai/Pai, respectively; $p < 0.05$; Fig. 1), similar to our previous study in male mice [3]. However, this bodyweight difference disappeared from five weeks of age onwards.

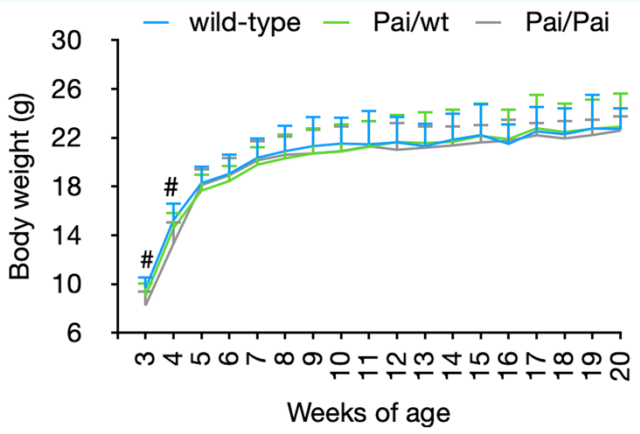

Figure 1. Comparison of growth of wild-type and Pai mice. Each group contained 11-29 mice. Bars represent the mean ± SD. # indicates $p < 0.05$ among three genotypes.

3. 3. Energy metabolism and activity studies

Energy metabolism and activity parameters were assessed in consideration of body weight. Compared to their wt littermates, both Pai/wt and Pai/Pai mice exhibited no significant differences in body weight gain, food and water intake (Fig. 2 A-C), total distance travelled during the whole 72-h observation (Fig. 2 D), and respiratory exchange ratio (Fig. 2 E-F). However, the other parameters showed varying differences.

The Pai/Pai mice covered a longer distance per sampling duration (~50% longer) and exhibited 52.5% higher speed during the light phase ($p < 0.05$; Fig. 2 G-H) but did not decrease their total locomotor activities in either the centre (Fig. 2 I-L) or margin/corners (Fig. 2 M-P). Nevertheless, during both the light ($p < 0.05$) and dark ($p > 0.05$) periods, they consumed 8.9% and 9.2% less O_2 (Fig. 2 Q) and produced 10.8% and 10.1% less CO_2 (Fig. 2 R) as well as 9.3% and 9.4% less heat (Fig. 2 S-T), respectively. The results suggest that Pai/Pai mice simultaneously reduce oxygen consumption and heat release while maintaining normal locomotor activities.

On the other hand, Pai/wt females did not reduce their central activities ($p > 0.05$; Fig. 2 I-L) but displayed 30.1% fewer marginal activities, such as marginal ambulating and stereotypic activities during the dark period ($p < 0.05$; Fig. 2 M-P). Moreover, during both the light and dark periods, they consumed 10.7% and 14.6% less O_2, produced 9.7% and 15.2% less CO_2, as well as 10.5% and 14.7% less heat, respectively ($p < 0.05$, Fig. 2 Q-T), suggesting that Pai/wt mice simultaneously reduce oxygen consumption and heat release while exhibiting fewer marginal activities.

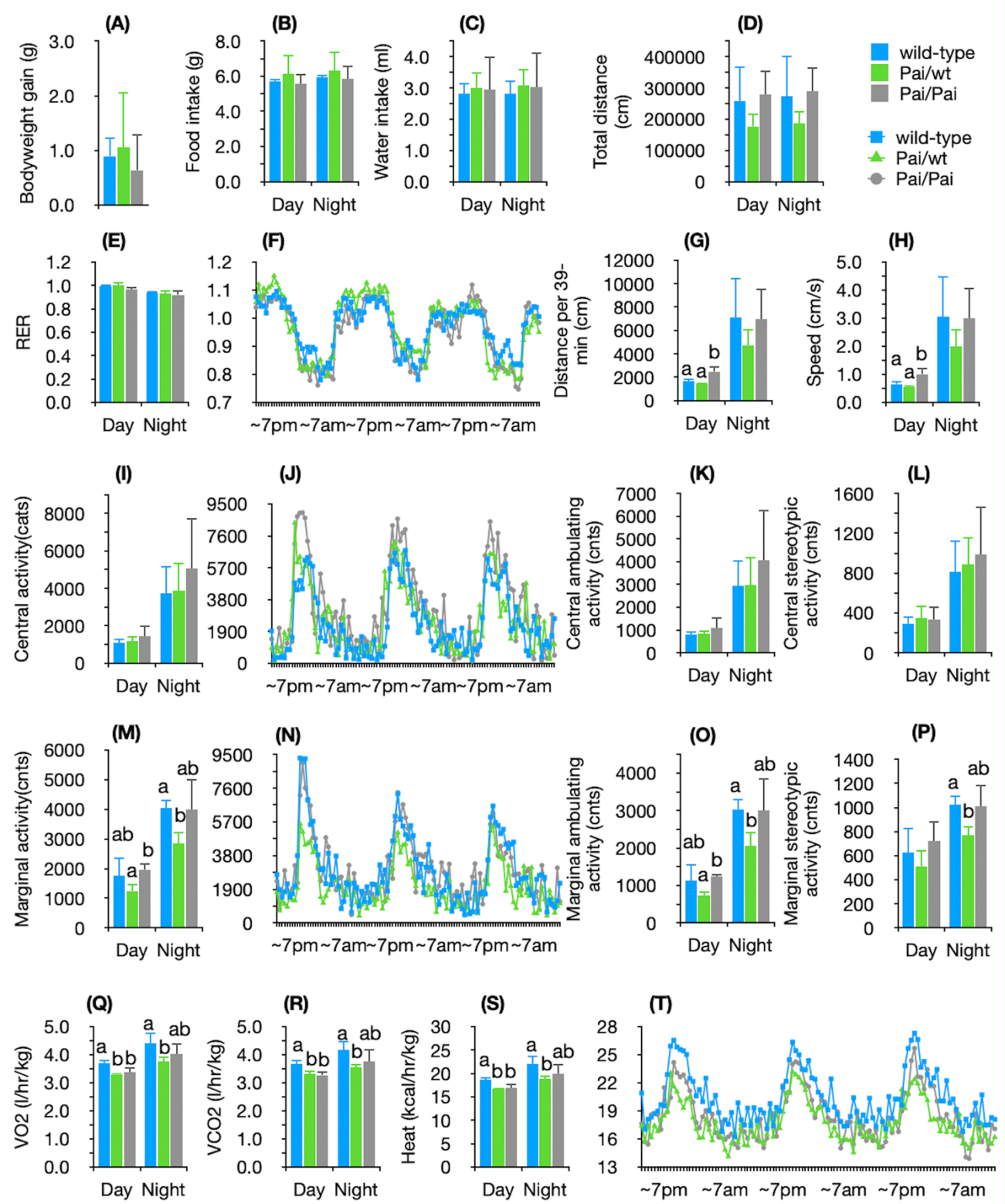

Figure 2. Abnormal energy metabolism and activities in Pai mice. Comparison of body weight gain during a 72-h period (A), food intake (B), water intake (C), total distance travelled during a 72-h period (D), respiratory exchange ratio (RER) and RER time course (E-F), distance travelled during a 39-min sampling duration (G), speed (H), locomotor activities in the centre of the cage and its time course (I-J), central ambulating and stereotypic activities

177 (K-L), locomotor activities in the margin or corners of the cage and its time course (M-N),
178 marginal ambulating and stereotypic activities (O-P), O_2 consumption (Q), CO_2 production
179 (R), heat release and its time course (S-T) among wild-type (n = 4), Pai/wt (n = 4) and Pai/Pai
180 (n = 4) mice at 11 weeks. The lights turned on and off at 7:00 am and 7:00 pm, respectively.
181 The data are normalised to lean body weight. The bars represent the mean ± SD. Different
182 letters indicate $p < 0.05$ within the same phase.

183

184 ***3. 4. Metabolic complications***

185 Concentrations of circulating glucose, insulin, leptin, and ghrelin (Table 3), as well as
186 small intestine length (Supplementary Table 2), showed no significant differences ($p > 0.05$)
187 between Pai mice and their wt littermates. This suggests that t10c12-CLA did not have any
188 significant impact on energy intake, which is consistent with the observation in the metabolic
189 cage.

Table 3. Circulating factors in wild-type and Pai mice

	wild-type (n)	Pai/wt (n)	Pai/Pai (n)
Blood glucose (mM)	7.35 ± 0.70 (12)	7.37 ± 1.18 (15)	7.55 ± 1.35 (13)
Serum insulin (μg/L)	0.21 ± 0.08 (9)	0.27 ± 0.11 (17)	0.32 ± 0.18 (8)
Serum leptin (μg/L)	1.04 ± 0.41 (8)	0.92 ± 0.21 (14)	0.91 ± 0.31 (7)
Serum ghrelin (ng/L)	181 ± 44 (7)	225 ± 108 (20)	210 ± 152 (6)
Serum fibroblast growth factor 21 (ng/L)	403 ± 29^{a} (16)	441 ± 49^{b} (10)	421 ± 34^{ab} (18)
Serum total cholesterol (μM)	311 ± 40 (17)	324 ± 40 (8)	321 ± 30 (16)
Plasma triglycerides (mg/dL)	107 ± 35^{a} (34)	105 ± 27^{a} (29)	129 ± 42^{b} (29)
Plasma high-density lipoprotein (mg/dL)	48.6 ± 13.9 (34)	47.7 ± 16.2 (29)	52.5 ± 19.6 (29)
Serum free fatty acids (μM)	471 ± 95 (8)	527 ± 79 (16)	517 ± 136 (8)
Serum Estradiol (pM)	71.0 ± 8.8 (15)	64.9 ± 6.8 (7)	68.4 ± 8.1 (15)
Serum prostaglandin E2 (ng/L)	349 ± 33^{a} (16)	356 ± 38^{ab} (8)	380 ± 38^{b} (16)
Serum glucagon (mU/L)	54.3 ± 62.3^{a} (20)	55.0 ± 38.4^{a} (17)	104 ± 67^{b} (16)
Serum cortosterone (μg/L)	7.51 ± 1.27^{a} (16)	7.88 ± 1.64^{ab} (8)	8.68 ± 1.61^{b} (16)
Serum adrenaline (μg/L)	3.01 ± 1.64^{a} (7)	10.5 ± 9.4^{b} (14)	13.7 ± 7.5^{b} (7)
Serum interleukin-6 (ng/L)	24.7 ± 17.7^{a} (9)	47.8 ± 27.8^{b} (14)	60.6 ± 32.8^{b} (6)
Serum tumour necrosis factor α (ng/L)	69.1 ± 54.9^{a} (12)	174 ± 161^{b} (16)	205 ± 175^{b} (13)
Serum C reactive protein (μg/L)	34.3 ± 19.2^{a} (16)	49.1 ± 31.4^{a} (17)	107 ± 72^{b} (10)
Serum lactate dehydrogenase (U/L)	2592 ± 646 (7)	2234 ± 627 (7)	2518 ± 454 (6)

Note: Blood samples were collected from non-fasted mice at the ages of 3 (specific for estradiol) or 11~15 weeks. Each value represents the mean ± SD and the numbers in brackets indicate the size of the tested samples. Different letters in superscript indicate a level of statistical significance of $p < 0.05$.

190

Although the circulating levels of total cholesterol, free FAs, high-density lipoprotein (HDL), and estradiol showed no significant differences among the three genotypes, the levels of plasma triglycerides (TGs) were significantly elevated in Pai/Pai mice when compared to wt or Pai/wt genotypes ($p < 0.05$, Table 3), indicating hypertriglyceridemia in Pai/Pai mice.

In Pai/Pai mice, serum concentrations of prostaglandin E2 (PGE2, 109%), glucagon (2-fold), corticosterone (116%), adrenaline (4.5-fold), tumour necrosis factor-alpha (TNFα, 3-fold), interleukin-6 (IL-6, 2.5-fold), and C-reactive protein (CRP, 3-fold) were significantly increased ($p < 0.05$) when compared to their wt littermates. However, only FGF21 (109%), adrenaline (3.5-fold), TNFα (2.5-fold), and IL-6 (2-fold) were significantly ($p < 0.05$) elevated in Pai/wt mice (Table 3). Additionally, there was no increase in blood levels of lactic acid dehydrogenase in either Pai mice, indicating no cellular injury caused by the PAI protein. These results suggest that the t10c12-CLA can lead to an inflammation reaction and response to illness-related stimuli in female mammals.

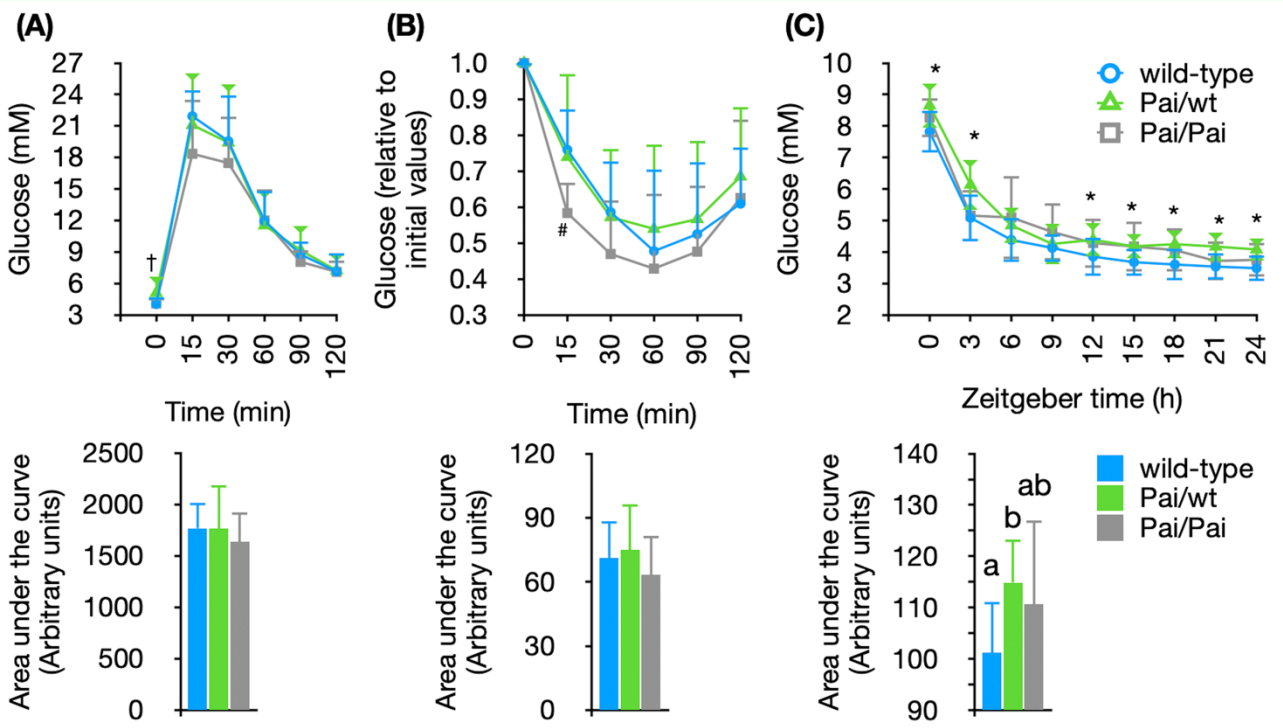

Figure 3. Comparisons of glucose (A) and insulin (B) tolerance tests and dynamic glucose levels (C) in wild-type (wt) and Pai mice. (A) Absolute blood glucose levels and the area under the curve are compared among wt (n = 5), Pai/wt (n = 10), and Pai/Pai (n = 5) mice. (B) Blood glucose levels relative to initial values and the area under the curve are compared among wt (n = 10), Pai/wt (n = 12), and Pai/Pai (n = 7) mice. (C) Dynamic blood glucose levels and the area under the curve are measured in wt (n = 12), Pai/wt (n = 13), and Pai/Pai (n = 10) fasting mice starved from Zeitgeber time 0 to 24. Zeitgeber times 0 and 12

are lights-on and -off times, respectively. The bars represent the mean ± SD. † indicates $p < 0.05$ between Pai/wt and wt or Pai/Pai mice; # indicates $p < 0.05$ between wt and Pai/Pai mice; * indicates $p < 0.05$ between wt and Pai/wt mice.

Both glucose and insulin tolerance tests showed no difference in the circulating glucose concentrations or the area under the curve between wt and two Pai genotypes. However, the glucose levels before glucose injection were significantly ($p < 0.05$) higher in Pai/wt mice compared to wt or Pai/Pai littermates (Fig. 3 A-B). To investigate further, we measured blood glucose levels during a 24-h fasting duration and found that Pai/wt mice maintained higher glucose levels continuously compared to their wt littermates ($p < 0.05$; Fig. 3 C). This suggests that t10c12-CLA can ameliorate the circulating glucose level in Pai/wt mice during starvation, which may be associated with the elevated FGF21 exclusively in Pai/wt female mice (Table 3), similar to high FGF21 levels in Pai/wt male mice [3], for its beneficial insulin-sensitising and glucose-lowering effects [17].

3. 5. WAT characteristics

WAT features were determined in the mice at 11 weeks of age. Compared to their wt littermates, Pai/Pai mice showed generalised organomegaly, including significantly enlarged livers, spleens, hearts, and ovaries, when body weight was considered ($p < 0.05$; Supplementary Table 2). However, no fat mass loss was observed (Fig. 4 A-B). The histological analysis did not reveal any changes in the cross-sectional area of white adipocytes (Fig. 4 C-D). Pai/wt mice showed enlarged ovaries only and no fat loss whereas its cross-sectional area per adipocyte was increased ($p < 0.05$), which was also confirmed by the increased mRNA level of leptin (Fig. 4 E).

Total RNA levels of 14 (42%) genes, including seven up-regulated and seven down-regulated, were changed in Pai/Pai white adipocytes among 33 examined genes (Table 4). The seven up-regulated genes were corticosterone receptor Nr3c1, F4/80, Adiponectin, G6p, Fasn, Ppar-γ, and Hsl. The seven down-regulated genes were Lpl, Cpt1a, Plin1, Prdm16, Insr, Glut4, and Chrebp. These aberrant gene expressions in white adipocytes suggest that t10c12-CLA can affect a series of metabolic processes, such as lipid metabolism, lipid and glucose uptake, energy expenditure, stimuli response and glucose homeostasis.

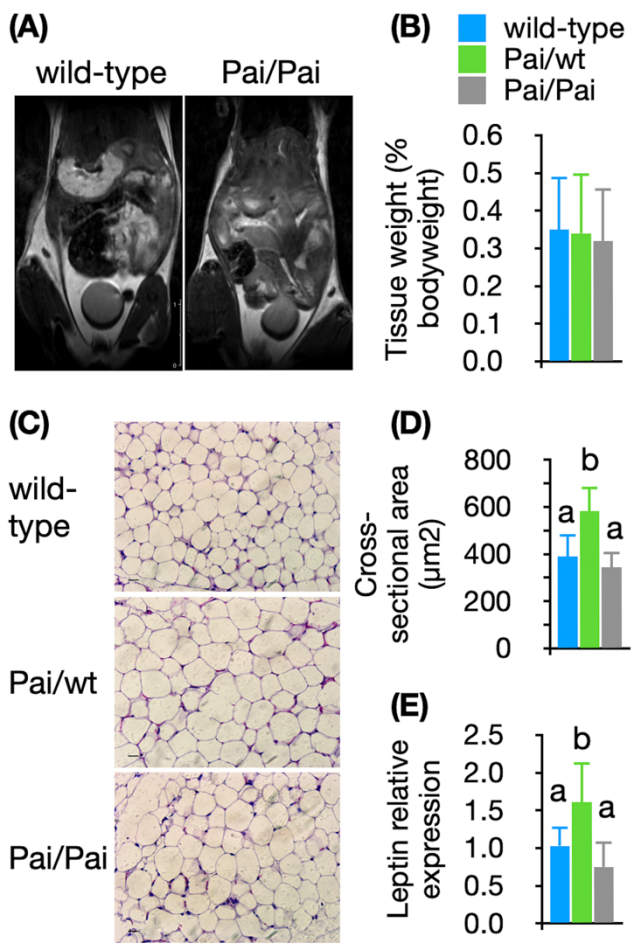

Figure 4. Magnetic resonance imaging and histological analysis of white adipose tissues. (A) Coronal sections were obtained on the whole-body midsection for four wild-type or Pai/Pai mice at 11 weeks in each group during magnetic resonance imaging (bar = 1 cm). The wild-type mice show adipose tissue in the subcutaneous and intra-abdominal regions as areas of increased signal intensity on images. The Pai/Pai mice show normal body fat. (B) There is no difference in WAT mass among wild-type (n = 21), Pai/wt (n = 17), and Pai/Pai (n = 13) mice. (C) Imaging of hematoxylin-eosin staining (bar = 10 μm), (D) analysis of cross-sectional area per cell, and (E) RNA level of leptin gene show that the volume of white adipocytes is specifically increased in Pai/wt mice (n = 5). The bars represent the mean ± SD. Different letters indicate $p < 0.05$.

Similar to Pai/Pai cells, Ppar-γ (1.52 ± 0.34, n = 10), Nr3c1 (1.53 ± 0.21, n = 12), and F4/80 (1.98 ± 0.64, n = 10) were also up-regulated ($p < 0.05$), and Cpt1a (0.58 ± 0.27, n = 5) and Chrebp (0.43 ± 0.45, n = 5) were down-regulated in Pai/wt adipocytes compared to wt samples ($p < 0.05$), respectively. The RNA levels of Fasn and Adiponectin were not different from those of wt samples ($p > 0.05$).

Table 4. Relative Expression of mRNAs in the white adipose tissue

Genes	Wild-type	Pai/Pai
Fatty acid synthase (*Fasn*)	1.04 ± 0.30 (6)	1.80 ± 0.47*** (8)
Peroxisome proliferator-activated receptor-γ (*Ppar-γ*)	1.03 ± 0.24 (12)	1.54 ± 0.61* (10)
Adipose triglyceride lipase (*Atgl*)	1.01 ± 0.16 (7)	1.06 ± 0.19 (7)
Hormone-sensitive lipase (*Hsl*)	1.02 ± 0.23 (9)	1.44 ± 0.29* (8)
Monoacylglycerol lipase (*Mgl*)	0.93 ± 0.25 (9)	0.99 ± 0.32 (8)
Perilipin 1a (*Plin1*)	1.07 ± 0.44 (8)	0.43 ± 0.16** (8)
Comparative gene identification 58 (*Cgi58*)	1.04 ± 0.30 (8)	0.81 ± 0.35 (8)
Lipoprotein lipase (*Lpl*)	1.03 ± 0.27 (14)	0.69 ± 0.24** (15)
Carnitine palmitoyltransferase Ia (*Cpt1a*)	1.06 ± 0.36 (8)	0.56 ± 0.15** (8)
Long-chain acyl-CoA dehydrogenase (*Lcad*)	1.12 ± 0.58 (7)	0.95 ± 0.44 (8)
Medium-chain acyl-CoA dehydrogenase (*Mcad*)	1.01 ± 0.17 (6)	1.07 ± 0.18 (9)
Uncoupling protein 1 (*Ucp1*)	1.09 ± 0.50 (6)	5.39 ± 5.88 (7)
Ppar-gamma coactivator 1 alpha (Pgc1α)	1.05 ± 0.39 (8)	1.18 ± 0.37 (8)
PR domain containing 16 (*Prdm16*)	1.01 ± 0.17 (7)	0.70 ± 0.20** (7)
Insulin receptor (*Insr*)	1.03 ± 0.25 (11)	0.75 ± 0.22** (13)
Insulin receptor substrate-1 (*Irs1*)	0.98 ± 0.32 (15)	1.03 ± 0.34 (20)
Insulin receptor substrate-2 (*Irs2*)	1.17 ± 0.69 (5)	2.28 ± 1.29 (6)
Phosphoinositide 3-kinase (*Pi3k*)	1.05 ± 0.39 (5)	0.78 ± 0.37 (8)
IGF binding protein 1 (*Igfbp1*)	1.80 ± 2.00 (6)	0.55 ± 0.14 (5)
Glucose transporter type 4 (*Glut4*)	1.02 ± 0.24 (6)	0.72 ± 0.17* (6)
Carbohydrate response element binding protein (Chrebp)	1.11 ± 0.51 (8)	0.35 ± 0.17** (8)
Fibroblast growth factor 21 (*Fgf21*)	1.08 ± 0.46 (6)	0.71 ± 0.39 (7)
Glucose-6-phosphatase (*G6p*)	1.24 ± 0.87 (6)	2.68 ± 0.83* (6)
Phosphoenolpyruvate carboxykinase (*Pepck*)	1.07 ± 0.42 (8)	1.11 ± 0.42 (8)
AMP-activated protein kinase (*Ampk*)	1.10 ± 0.49 (5)	1.45 ± 0.58 (8)
Adiponectin	0.99 ± 0.24 (9)	1.42 ± 0.38** (10)
Nuclear receptor subfamily 3 group C member 1 (*Nr3c1*)	1.04 ± 0.29 (22)	1.64 ± 0.81** (22)
F4/80	1.03 ± 0.29 (12)	1.54 ± 0.58* (11)
CD68	1.06 ± 0.38 (14)	1.03 ± 0.61 (13)
CD11c	1.05 ± 0.29 (14)	0.95 ± 0.44 (16)
CCAAT/enhancer-binding-protein beta (*Cebp*)	1.04 ± 0.31 (6)	1.13 ± 0.60 (8)
Forkhead box protein c2 (*Foxc2*)	1.02 ± 0.21 (5)	1.15 ± 0.45 (7)
Pai	1.24 ± 1.23 (23)	393 ± 270*** (25)

Numbers in brackets indicate the size of tested samples. Each value represents the mean ± SD. * indicates $p < 0.05$; ** indicates $p < 0.01$; *** indicates $p < 0.001$, respectively.

261

262 ***3. 6. BAT thermoregulation***

263 To investigate the possible reason for hypothermia in Pai/Pai mice, BAT features
264 were measured. Magnetic resonance imaging and dissection analysis did not reveal any mass
265 changes of BAT in Pai mice (Fig. 5 A-B). HE staining showed Pai/Pai adipocytes with
266 uniform and small-sized lipid drops, while Pai/wt adipocytes had size-irregular lipid drops
267 compared to wt adipocytes containing uniform and large-sized lipid drops (Fig. 5 C). The

268 reduced cross-sectional areas per adipocyte indicated that the volumes of brown adipocytes
269 decreased significantly in both Pai genotypes ($p < 0.05$; Fig. 5 D).

270

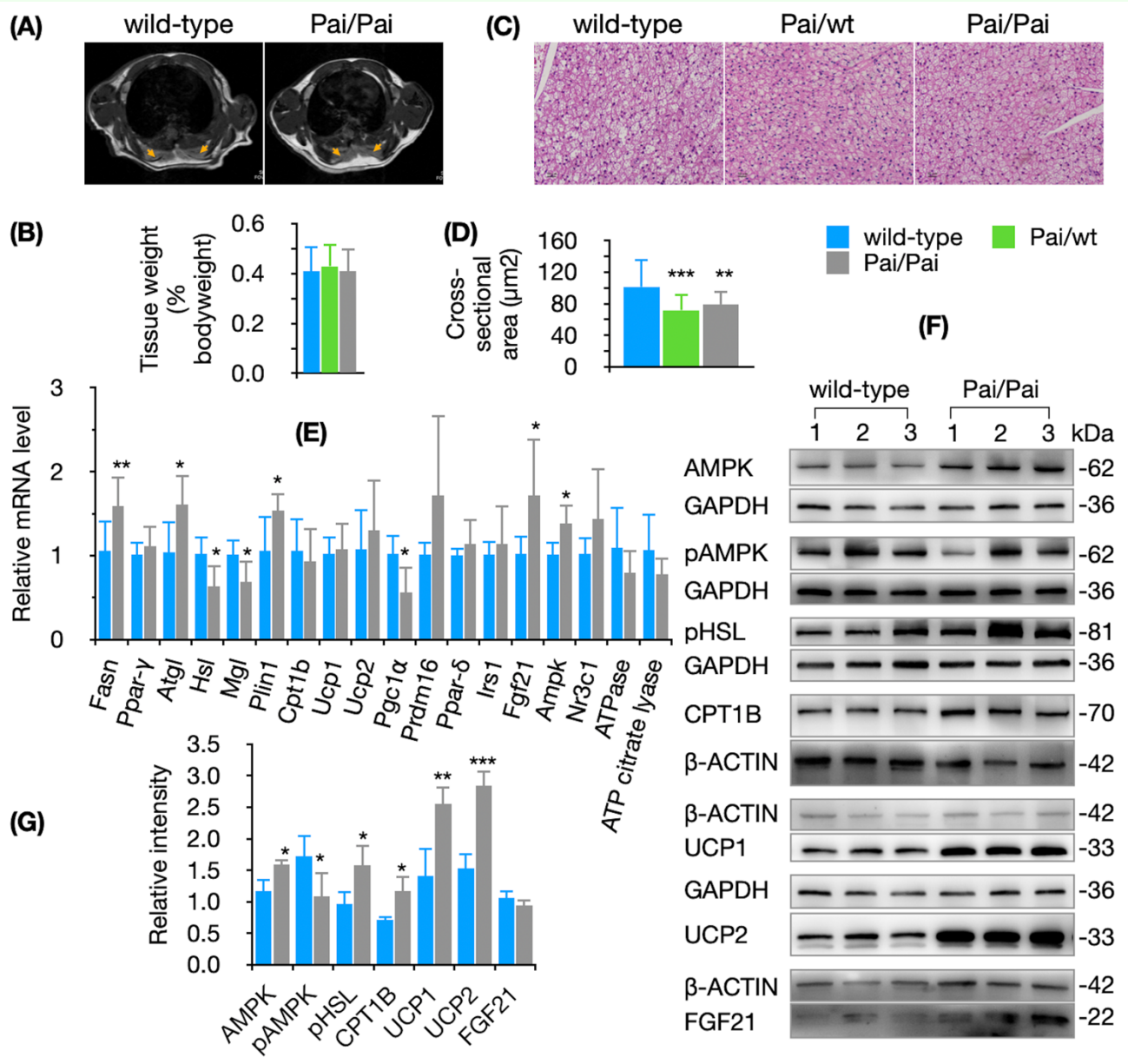

271

272 **Figure 5. Aspects of brown adipose tissues.** (A) Axial sections of the interscapular BAT
273 show similar areas of grey signal intensity on magnetic resonance images (brown arrows)
274 between four Pai/Pai and four wild-type mice at 11 weeks. (B) There is no BAT mass
275 difference among wild-type (n = 21), Pai/wt (n = 17), and Pai/Pai (n = 13) mice. (C-D)
276 Analysis of hematoxylin-eosin staining shows that the sizes of lipid drops become small in
277 the Pai/wt or Pai/Pai adipocytes (bar = 10 μm) and the cross-sectional area per cell is
278 decreased in Pai/wt and Pai/Pai mice (n = 5). (E) Analyses of the relative expression of
279 mRNAs of critical genes in wild-type (n = 5~6) and in Pai/Pai (n = 6~8) mice. (F-G) Western

280 blot analysis of proteins and their relative intensities in wild-type (n = 3) and Pai/Pai mice
281 (n = 3). See Table 4 for full names of genes/proteins. pAMPK, phosphorylated AMPK; pHSL,
282 phosphorylated hormone-sensitive lipase. The bars represent the mean ± SD. * indicates $p <$
283 0.05; ** indicates $p < 0.01$; and *** indicates $p < 0.001$ vs. wild-type, respectively.

284

285 In Pai/Pai brown adipocytes, among the 18 tested genes, the transcriptional levels
286 were changed in eight genes, which were up-regulated Fasn, Atgl, Plin1, Fgf21, and Ampk,
287 as well as down-regulated Hsl, Mgl, and Pgc1α ($p < 0.05$; Fig. 5 E). In contrast, the other
288 critical genes involved in lipolysis and thermogenesis, such as Ppar-γ, Ucp1, Ucp2, Prdm16,
289 and Ppar-δ, showed no changes in RNA levels. Western blot analysis revealed that UCP1
290 and UCP2, phosphorylated HSL and CPT1B were over-expressed ($p < 0.05$; Fig. 5 F-G).
291 Simultaneously, an increase in total AMPK and a decrease in phosphorylated AMPK were
292 observed in Pai/Pai BAT. These results indicate that the t10c12-CLA effect is associated with
293 BAT's thermogenesis, lipolysis, and beta-oxidation processes. The discrepancy of levels of
294 some mRNA and their encoded proteins also suggests the complex regulation by feedback
295 or adaptive response.

296

297 ***3. 7. Hepatic features***

298 To investigate if t10c12-CLA affects hepatic function, we compared the Pai liver
299 features and the molecular basis of lipid and glucose metabolism with wt samples.

300 In Pai/Pai mice, hepatic hypertrophy was observed (Fig. 6 A). The levels of hepatic
301 TC remained unchanged (Fig. 6 B), but the transcriptional levels of critical genes involved in
302 the sterol pathway were changed, which were down-regulated Srebp1a, Insig2, Hmgcr, and
303 Ldlr; as well as up-regulated Srebp1c and Insig1 ($p < 0.05$; Table 5). On the other hand, the
304 levels of hepatic TGs increased by 15.4%, and histological staining showed profound fat
305 accumulation (~2.3 fold) in swollen hepatocytes ($p < 0.05$; Fig. 6 C-G), indicating hepatic
306 steatosis in Pai/Pai mice. RNA levels of 48% (11/23) genes involved in lipid metabolism were
307 significantly ($p < 0.05$) altered in Pai/Pai livers, including three up-regulated (Fasn, Mgl,
308 Cgi58) and eight down-regulated genes, which were down-regulate Ppar-γ, Dgat1, Dgat2,
309 Atgl, Lpl, Cpt1a, Mcad, and Acox1; as well as up-regulated Mgl and Cgi58 (Table 5). Western
310 blot analysis revealed that the protein levels of pAMPK and FASN were reduced, and CPT1A
311 was increased while the levels of AMPK, ATGL, and CPA1B did not change (Fig. 6 H-I). The
312 result indicates that the chronic effect of t10c12-CLA attenuates the pathway modified by

pAMPK. It also suggests that hepatic steatosis causes the down-regulation of fatty acid synthesis and up-regulation of beta-oxidation through negative feedback regulation in the liver.

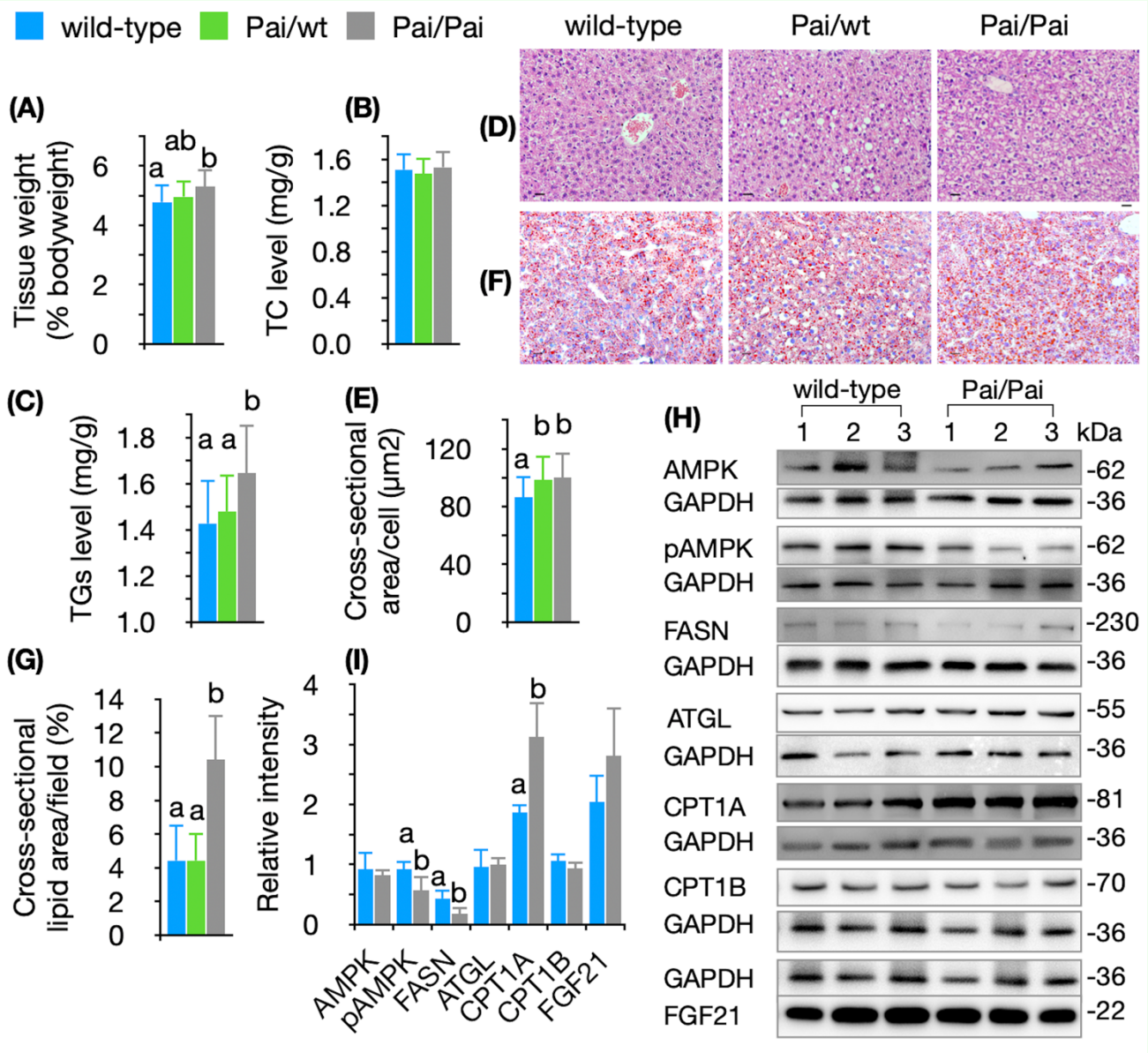

Figure 6. Lipid and histological analysis of livers. (A) Dissection analysis shows an increased liver mass in Pai/Pai (n = 13) but not in Pai/wt (n = 17) mice compared to wild-type mice (n = 21). (B-C) ELISA analyses indicate similar levels of hepatic total cholesterol (TC) and increased levels of triglycerides (TGs) in Pai/Pai livers (n = 12) compared to wild-type (n = 14) and Pai/wt (n = 14). (D-E) Analyses of hematoxylin-eosin staining show the abnormal morphology and hepatocyte oedema in Pai/Pai livers and the enlarged cross-sectional area per cell in Pai/Pai and Pai/wt hepatocytes compared to wild-type samples (n

325 = 5). (F-G) Analyses of Oil red staining show hepatic lipid accumulation in Pai/Pai but not
326 in Pai/wt mice compared to wild-type mice (n = 5), Bar = 10 μm. (H-I) Western blot analysis
327 of proteins and their relative intensities in wild-type (n=3) and Pai/Pai mice (n = 3). The bars
328 represent the mean ± SD, and different letters indicate $p < 0.05$.

329

330 Moreover, this study analysed a range of crucial enzymes related to insulin/IGF
331 signalling and glucose metabolism. The mRNA levels of Igfbp1, Glut4, Fgf21, G6p, and Pepck
332 were decreased, but western blot analysis showed that the FGF21 level did not alter. These
333 findings suggest that t10c12-CLA may have a significant impact on glucose metabolism and
334 insulin sensitivity at least on transcriptional levels in female livers. Additionally, two
335 NADPH-producing enzymes, Malic and Pgd, were significantly up-regulated, and the
336 inflammatory factor CD11c was down-regulated in the Pai/Pai livers ($p < 0.05$; Table 5).

337

Table 5. Relative Expression of mRNAs in the liver

Genes	**wild-type**	**Pai/wt**	**Pai/Pai**
Sterol pathway			
Liver X receptor α (*Lxr*α)	1.00 ± 0.09 (6)	0.91 ± 0.26 (6)	1.08 ± 0.45 (8)
Liver X receptor β (*Lxrβ*)	1.04 ± 0.31 (9)	0.91 ± 0.42 (6)	1.11 ± 0.26 (7)
SREBP cleavage-activating protein (*Scap*)	1.01 ± 0.15 (8)	0.92 ± 0.15 (6)	0.90 ± 0.25 (6)
Sterol Regulatory Element Binding Protein-1a (*Srebp1a*)	1.02 ± 0.22^{a} (7)	0.46 ± 0.25^{b} (6)	0.61 ± 0.20^{b} (7)
Srebp1c	0.96 ± 0.33^{a} (6)	1.61 ± 0.55^{b} (7)	1.60 ± 0.42^{b} (5)
Srebp2	1.07 ± 0.39 (8)	1.06 ± 0.22 (7)	1.25 ± 0.52 (8)
Insulin induced gene 1 (*Insig1*)	1.03 ± 0.25^{a} (7)	1.97 ± 0.52^{b} (7)	1.47 ± 0.26^{b} (5)
Insulin induced gene 2a (*Insig2*)	1.07 ± 0.38^{a} (6)	0.20 ± 0.34^{b} (6)	0.59 ± 0.31^{b} (5)
HMG-CoA reductase (*Hmgcr*)	1.01 ± 0.16^{a} (6)	1.23 ± 0.32^{a} (5)	0.62 ± 0.34^{b} (6)
LDL receptor (*Ldlr*)	1.04 ± 0.33^{a} (8)	1.23 ± 0.36^{a} (6)	0.71 ± 0.10^{b} (5)
Fatty acid and TGs synthesis			
Fatty acid synthase (*Fasn*)	1.01 ± 0.18^{a} (6)		2.65 ± 1.32^{b} (6)
Stearoyl-CoA desaturase 1 (*Scd1*)	1.07 ± 0.43 (7)	0.97 ± 0.49 (6)	1.11 ± 0.57 (6)
Peroxisome proliferator-activated receptor-γ (*Ppar-γ*)	1.01 ± 0.46^{a} (14)	1.06 ± 0.27^{a} (7)	0.66 ± 0.44^{b} (12)
Glycerol-3-phosphate acyltransferase 1 (*Gpat1*)	1.04 ± 0.33 (7)	1.44 ± 0.46 (6)	1.22 ± 0.31 (6)
1-acylglycerol-3-phosphate O-acyltransferase 2 (*Agpat2*)	0.97 ± 0.25 (8)	0.80 ± 0.22 (6)	1.11 ± 0.31 (7)
Diacylglycerol acyltransferase-1 (*Dgat1*)	1.00 ± 0.16^{a} (7)	0.81 ± 0.18^{ab} (6)	0.70 ± 0.13^{b} (7)
Diacylglycerol acyltransferase-2 (*Dgat2*)	1.00 ± 0.08^{a} (6)	1.04 ± 0.15^{a} (6)	0.85 ± 0.11^{b} (5)
CD36 (Cd36)	1.06 ± 0.41 (6)		0.83 ± 0.31 (6)

Table 5. Relative Expression of mRNAs in the liver

Genes	wild-type	Pai/wt	Pai/Pai
Lipolysis and fatty acid oxidation			
Hepatic triglyceride lipase (*Htgl*)	0.98 ± 0.27 (7)	0.90 ± 0.28 (6)	1.13 ± 0.34 (7)
Adipose triglyceride lipase (*Atgl*)	1.02 ± 0.21[a] (6)	0.79 ± 0.36[ab] (6)	0.56 ± 0.14[b] (6)
Hormone-sensitive lipase (*Hsl*)	1.05 ± 0.33 (8)	1.29 ± 0.41 (6)	1.16 ± 0.49 (8)
Monoacylglycerol lipase (*Mgl*)	1.02 ± 0.19[a] (8)	1.65 ± 0.55[b] (6)	1.56 ± 0.58[b] (7)
Comparative gene identification 58 (*Cgi58*)	1.05 ± 0.34[a] (7)	1.38 ± 0.66[ab] (6)	1.75 ± 0.59[b] (7)
Adenylate cyclase 3 (*Adcy3*)	1.07 ± 0.42 (8)		1.08 ± 0.23 (8)
Lipoprotein lipase (*Lpl*)	1.02 ± 0.23[a] (7)	0.60 ± 0.17[b] (6)	0.50 ± 0.23[b] (6)
Carnitine palmitoyltransferase Ia (*Cpt1a*)	1.01 ± 0.19[a] (14)	0.83 ± 0.17[b] (7)	0.68 ± 0.18[b] (11)
Long-chain 3-hydroxyacyl-CoA dehydrogenase (*Lchad*)	1.04 ± 0.28 (9)		1.01 ± 0.25 (9)
Acetyl-CoA acyltransferase 2 (*Acaa2*)	1.08 ± 0.44 (7)		1.23 ± 0.23 (6)
Long-chain acyl-CoA dehydrogenase (*Lcad*)	1.00 ± 0.09 (8)	0.93 ± 0.22 (7)	0.78 ± 0.30 (8)
Medium-chain acyl-CoA dehydrogenase (*Mcad*)	1.03 ± 0.27[a] (9)	0.57 ± 0.12[b] (6)	0.65 ± 0.20[b] (6)
Uncoupling protein 1 (*Ucp1*)	1.04 ± 0.32 (7)	1.12 ± 0.40 (7)	0.98 ± 0.34 (7)
Acyl-CoA oxidase-1 (*Acox1*)	1.04 ± 0.32[a] (8)	0.89 ± 0.32[a] (7)	0.69 ± 0.32[b] (8)
Acyl-CoA oxidase-2 (*Acox2*)	1.07 ± 0.42 (9)		1.17 ± 0.43 (9)
Insulin and IGF-1 signaling			
Insulin receptor (*Insr*)	1.05 ± 0.37 (9)	1.35 ± 0.42 (6)	1.36 ± 0.70 (8)
Insulin receptor substrate-1 (*Irs1*)	0.97 ± 0.43 (6)	0.97 ± 0.43 (4)	0.94 ± 0.59 (6)
Insulin receptor substrate-2 (*Irs2*)	1.27 ± 1.01 (9)	1.27 ± 0.87 (7)	1.41 ± 0.99 (8)
Phosphoinositide 3-kinase (*Pi3k*)	1.04 ± 0.28 (7)		1.17 ± 0.24 (7)
Insulin-like growth factor-1 (*Igf1*)	1.04 ± 0.31[a] (8)	1.16 ± 0.29[a] (7)	2.09 ± 0.80[b] (6)
IGF binding protein 1 (*Igfbp1*)	1.04 ± 0.30[a] (6)	0.45 ± 0.33[b] (6)	0.09 ± 0.02[b] (5)
Forkhead box protein a2 (*Foxa2*)	1.06 ± 0.37[a] (9)	1.98 ± 0.86[b] (6)	1.76 ± 0.48[b] (7)
Glucose metabolism and gluconeogenesis			
Glucose transporter type 4 (*Glut4*)	1.06 ± 0.38[a] (6)	0.88 ± 0.28[a] (5)	0.61 ± 0.25[b] (6)
Carbohydrate response element binding protein (*Chrebp*)	1.03 ± 0.26 (5)		1.33 ± 0.43 (6)
Fibroblast growth factor 21 (*Fgf21*)	1.07 ± 0.46[a] (5)		0.19 ± 0.12[b] (7)
Glucose-6-phosphatase (*G6p*)	1.07 ± 0.41[a] (9)	0.47 ± 0.17[b] (7)	0.66 ± 0.19[b] (6)
Phosphoenolpyruvate carboxykinase (*Pepck*)	1.04 ± 0.29[a] (8)	0.53 ± 0.22[b] (6)	0.51 ± 0.19[b] (7)
NADPH-producing			
Malic enzyme (*Malic*)	0.99 ± 0.32[a] (8)	0.98 ± 0.39[a] (7)	1.72 ± 0.70[b] (7)
Glucose-6-phosphate dehydrogenase (*G6pd*)	1.06 ± 0.38 (6)	1.14 ± 0.34 (4)	1.05 ± 0.46 (4)
6-Phosphogluconate dehydrogenase (*Pgd*)	1.05 ± 0.35[a] (7)		1.73 ± 0.56[b] (6)
Others			
AMP-activated protein kinase (*Ampk*)	1.07 ± 0.41 (7)		1.48 ± 0.32 (7)
Liver kinase B1 (*Lkb1*)	1.02 ± 0.23 (5)		1.10 ± 0.12 (5)
Nuclear receptor subfamily 3 group C member 1 (*Nr3c1*)	1.07 ± 0.39 (6)		2.01 ± 1.05 (6)

Table 5. Relative Expression of mRNAs in the liver

Genes	wild-type	Pai/wt	Pai/Pai
CD11c	1.04 ± 0.31^{a} (7)	0.57 ± 0.26^{b} (6)	0.53 ± 0.27^{b} (7)
Cyclophilin	1.01 ± 0.17 (9)	1.04 ± 0.28 (6)	1.01 ± 0.16 (6)
Pai	1.01 ± 0.43^{a} (5)	1674 ± 569^{b} (6)	6059 ± 2317^{c} (6)

Numbers in brackets indicate the size of tested samples. Each value represents the mean ± SD. Different letters in superscript indicate $p < 0.05$.

338

339 Compared to wt samples, Pai/wt livers exhibited normal except for swollen cells
340 (Fig. 6 E). However, among the forty tested genes (Table 5), the mRNA levels of eight genes
341 (Hmgcr, Ldlr, Ppar-γ, Dgat2, Acox1, Igf1, Glut4, and Malic) were significantly ($p < 0.05$)
342 different from those in Pai/Pai livers, but not different from those in wt samples. The
343 remaining 32 genes had similar transcription levels to Pai/Pai samples, and 13 (33%) of them
344 were markedly different from those in wt samples ($p < 0.05$). Specifically, these 13 genes that
345 exhibited different expressions from wt livers included four up-regulated (Mgl, Srebp1c,
346 Insig1, and Foxa2) and nine down-regulated (Lpl, Cpt1a, Mcad, Srebp1a, Insig2, Igfbp1, G6p,
347 Pepck, and Cd11c). These results suggest that gene expression is genotype-specific and that
348 the process of lipolysis and gluconeogenesis is impaired in Pai/wt mice.

349

350 ***3. 8. Hypothalamic analysis***

351 To determine whether t10c12-CLA affected the hypothalamus, critical hypothalamic
352 genes and proteins were also measured. The mRNA levels of the leptin receptor and agouti-
353 related peptide were increased, while the transcription levels of the ghrelin receptor and
354 Orexins decreased in the Pai/wt or Pai/Pai hypothalamus when compared to wt mice (Fig.
355 7 A). Western blot analysis revealed no changes in AMPK, phosphorylated AMPK, and
356 GRP78 proteins in the Pai/Pai hypothalamus; additionally, the ratio of pAMPK/AMPK did
357 not show a significant difference between wt and Pai/Pai samples ($p > 0.05$; Fig. 7 B-C). These
358 findings suggest that the central regulation of energy intake may only be affected at the
359 transcriptional level.

360

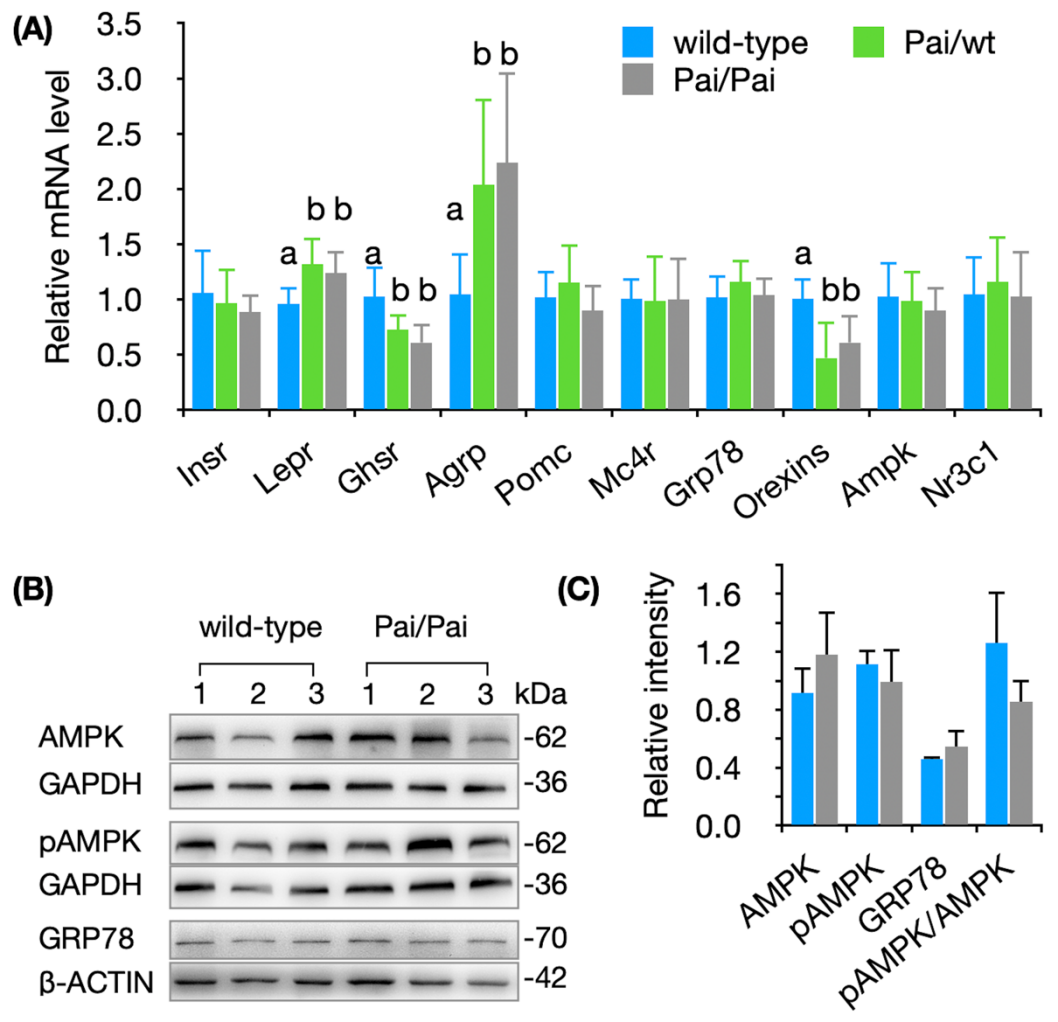

Figure 7. Analyses of the relative mRNAs (A), protein levels and their relative intensities in the hypothalamus (B-C). Agrp, Agouti-related peptide; Ampk, AMP-activated protein kinase; Ghsr, Ghrelin receptor; Grp78, glucose-regulated protein 78; Insr, Insulin receptor; Lepr, Leptin receptor; Mc4r, Melanocortic 4 receptor; Nr3c1, Nuclear receptor subfamily 3 group C member 1; (p)AMPK, (phosphorylated) AMP-activated protein kinase; Pomc, Proopiomelanocortin. The sample sizes for RNA analysis are 6~9 in each group. The bars represent the mean ± SD, and different letters indicate $p < 0.05$.

369 **4. DISCUSSION**

370

371 Our previous observation in Pai/Pai male mice showed that t10c12-CLA reduced
372 body fat by releasing heat via BAT activation with lower blood TGs [3]. Conversely, in the
373 Pai female mice, t10c12-CLA did not cause body fat loss but resulted in complicated
374 symptoms, including hypothermia, fatty liver and hypertriglyceridemia, and was highly
375 responsive to stress and inflammation in a dose-dependent manner. The different
376 physiological and pathological characteristics of both sexes can help us understand the
377 mechanism of action of t10c12-CLA in gender-specific and dose-dependent manners. As for
378 Pai mice, there are two problems we have not fixed until now. Firstly, we have reported as
379 many results as possible for a comprehensive understanding of the Pai mouse, but a few
380 parameters are difficult to explain well and even show contradictions in some respects.
381 Secondly, explaining why there are only minimal differences in t10c12-CLA and linoleic acid
382 is challenging although we once observed drastic changes in an increase of product t10c12-
383 CLA and a decrease of substrate linoleic acid in Pai-transfected 3T3 cells [18].

384 The metabolic pathway of t10c12-CLA, similar to that of linoleic or alpha-linolenic
385 acids [18], suggests it can competitively interrupt the metabolic pathway of n-6 or n-3 FAs
386 and their derived leukotrienes signals/hormonal molecules. It also indicates that t10c12-CLA
387 can be directly converted into the analogues of n-6 FAs and their derivatives. PGE2, an
388 arachidonic acid-derived hormone, will be easily disturbed by t10c12-CLA. PGE2 is involved
389 in stress response and has essential effects on inflammation, fever, and renal filtration [19]. It
390 can induce corticosterone secretion by regulating the hypothalamic-pituitary-adrenal axis
391 activity and enhancing adrenaline synthesis in the Chromaffin cells of the adrenal medulla.
392 Subsequently, the increased circulating corticosterone and adrenaline could stimulate excess
393 glucagon secretion [20]. In Pai/Pai female mice, we have observed the excess PGE2 induced
394 by t10c12-CLA, and then the PGE2 (or analogues) caused the increases in corticosterone,
395 glucagon, adrenaline, and inflammatory factors (IL-6, TNFα, and CRP). Obviously,
396 hypothermia in Pai/Pai female mice may be related to hyperprostaglandinemia,
397 hyperadrenerginemia and inflammatory response; while hyperglyceridemia and fatty liver
398 are associated with hypercorticosteroidemia and glucagon resistance.

399 In the hypothalamic preoptic area, PGE2 receptors EP3, coupled to cAMP decreases,
400 can stimulate a passive defence mechanism such as less O_2 consumption and hypothermia to
401 avoid further energy expenditure; while receptors EP4, connected to cAMP increases, can

402 stimulate an active defence mechanism, including more O_2 consumption and febrile
403 responses by increasing BAT thermogenesis, typically occurs to promote well-being and
404 survival [19,21]. It suggests that gender-based differences in PGE2 levels might partially result
405 in the opposite heat release in male and female Pai/Pai mice. In female mice, the co-elevation
406 of PGE2 and corticosterone suggests that t10c12-CLA induced a passive defence mechanism
407 including hypothermia which conversely promotes BAT thermogenesis and lipid
408 metabolism by negative feedback to down-regulate pAMPK and up-regulate UCP1, UCP2,
409 CPT1B, and pHSL. In contrast, in male mice, the lack of PGE2 elevation suggests that t10c12-
410 CLA induced an active defence mechanism including hyperthermia to promote survival [3].

411 In addition to PGE2- and adrenaline-induced heating [22], BAT thermogenesis can be
412 mediated through the central GRP78 [23,24] or AMPK-OREXINS-BMP8B pathway [25].
413 Orexin-null mice exhibited periods of decreased activity during the dark phase and
414 demonstrated hypothermia, reduced oxygen consumption, and blunted thermogenic
415 responses [26]; furthermore, BMP8B's thermogenic effect is sexually dimorphic and observed
416 in females only [25]. The Pai/Pai female mice exhibited similar phenotypes to orexin-null
417 mice and lower transcription levels of Orexins in the Pai hypothalamus. These characteristics
418 suggest that the t10c12-CLA-induced BAT thermogenesis may be regulated through central
419 pathways in female mice. Unfortunately, we did not observe evident changes in GRP78,
420 AMPK, pAMPK, and pAMPK/AMPK ratio in the hypothalamus.

421 Previous studies on mice have yielded conflicting results on whether dietary t10c12-
422 CLA leads to hepatic steatosis [11,16,27,28]. The current observation of fatty liver and
423 hypertriglyceridemia in Pai/Pai mice, which may be associated with t10c12-CLA-induced
424 excess corticosterone for the overproduction of corticosterone can lead to Cushing syndrome,
425 corticosteroid-induced lipodystrophy, hypertriglyceridemia, or hepatic steatosis [29,30]. On
426 the other hand, the existence of glucagon resistance can increase liver fat [31-33], although
427 chronic increases in plasma glucagon promote lipolysis through INSP3R1/CAMKII/ATGL
428 [34] or PKA/HSL pathways in hepatocytes [35] and stimulate beta-oxidation by activating
429 AMPK/PPAR-α/CPT1A/MCAD pathway [20]. In the current study, the serum glucagon
430 concentration increased nearly twofold in Pai/Pai female mice, which is similar to its
431 physiological levels (2~3 fold) in response to long-term fasting or hypoglycemia [36], whereas
432 the protein levels of unchanged ATGL, decreased pAMPK, and increased CPT1A indicate
433 the chronic glucagon excess did not stimulate the lipolysis and beta-oxidation in the liver.
434 These results suggest that the chronic impact of t10c12-CLA might give rise to glucagon
435 resistance in Pai/Pai female mice. In this case, the down-regulated hepatic enzymes may not

436 fully and immediately catalyse the FAs molecules mobilised from other tissues based on
437 glucagon stimulation. Consequently, it disrupts hepatic and systemic lipid homeostasis and
438 leads to dyslipidemia and fatty liver in female mice. Contrarily, the t10c12-CLA did not cause
439 the overproduction of corticosterone or glucagon in Pai/Pai male mice. Thus, the mice had
440 no fatty liver disease and even exhibited lower TGs levels in the blood.

441 FGF21 is a key regulator of the specific hormonal signalling pathway in increasing
442 energy expenditure, reducing hepatic and plasma TGs levels, accelerating lipoprotein
443 catabolism in WAT and BAT [37], and suppressing physical activity via central action [38].
444 FGF21 signalling enhances insulin sensitivity and lowers serum glucose by acting directly on
445 adipose tissues [17,39]. The Pai/wt mouse is the first animal in which t10c12-CLA can induce
446 FGF21 secretion. Excess FGF21 is a unique feature in Pai/wt, not in Pai/Pai genotypes,
447 indicating that t10c12-CLA-induced FGF21 secretion is specifically associated with low doses
448 in both genders and it can be suppressed to the normal levels through negative feedback
449 when high doses occur in Pai/Pai mice. This suggests that the health benefits of low-dose
450 t10c12-CLA may be due, in part, to its ability to stimulate FGF21 secretion. Therefore, the
451 different effects of t10c12-CLA on glucose metabolism in diabetic Zucker fatty rats [40] and
452 insulin resistance in mice [12,41] may be related to the different levels of FGF21 induced by
453 t10c12-CLA. In the current study, excess FGF21 may be associated with specific phenotypes
454 in Pai/wt mice, such as blood glucose homeostasis during starvation, enlarged white
455 adipocytes, no steatosis in hepatocytes and normal circulating TGs. The exact mechanism by
456 which t10c12-CLA activates FGF21 secretion remains unclear and requires further
457 investigation.

458 Based on the excesses of hormones, abnormality of the energy metabolism, and
459 physical activities in Pai/Pai mice in this study, we suggest that high doses of t10c12 result
460 in an increased PEG2 which subsequently induces increases in corticosterone, glucagon, and
461 adrenaline, and inflammatory factors (IL6, TNFα, and C reaction protein). The combination
462 of these factors causes metabolic syndrome, including fatty liver, hyperglyceridemia,
463 hypothermia, and inflammatory changes in lean female mice (Fig. 8). Conversely, low doses
464 of t10c12-CLA may cause increases in circulating adrenaline which can induce WAT lipolysis
465 and BAT heating through a mechanism of negative feedback, and FGF21 which can promote
466 energy expenditure, reduce hepatic and plasma TGs levels, accelerate lipoprotein catabolism
467 in adipocytes, suppress physical activity, and enhance insulin sensitivity and lower serum
468 glucose (Fig. 8).

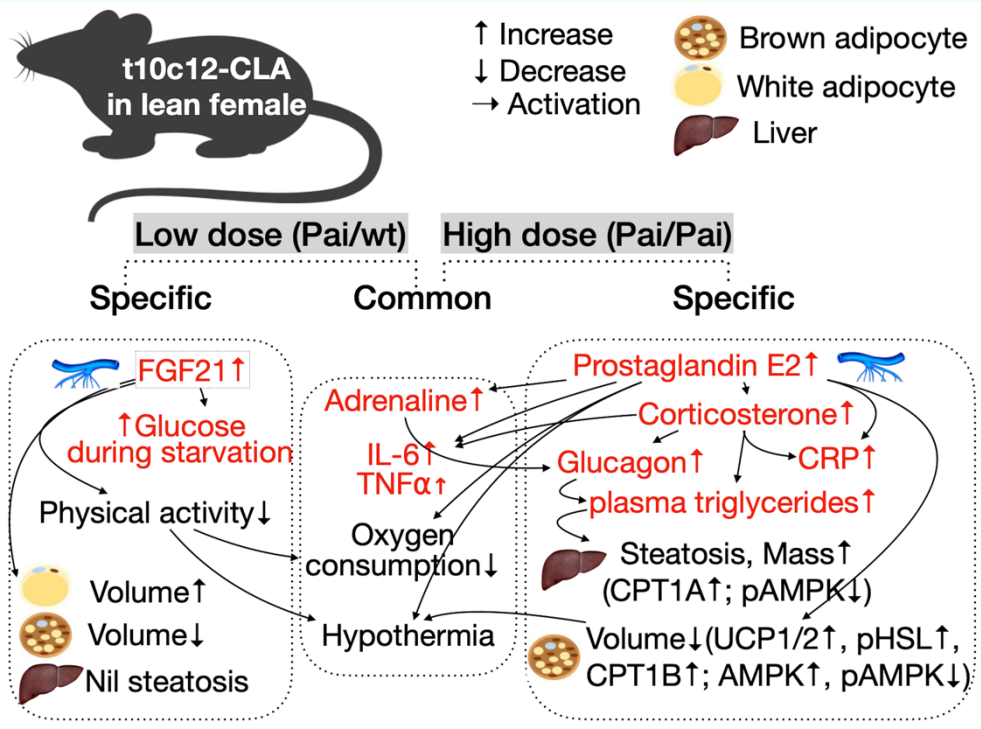

Figure 8. Diagram showing the dose-dependent effect of chronic t10c12-CLA on lean female mice. Besides the common effects, such as increased adrenaline, IL-6, and TNFα, as well as decreased heat release and oxygen consumption (Middle panel), the low doses specifically increase circulating levels of FGF21 which plays active roles in maintaining energy homeostasis, suppressing physical activity, and improving serum glucose levels in Pai/wt mice (Left panel). Conversely, the high doses specifically result in excesses of prostaglandin E2, corticosterone, glucagon, and CRP; subsequently, the combination of these factors causes metabolic syndrome, including hypothermia, fatty liver, and hypertriglyceridemia in Pai/Pai mice (Right panel). Words in black and red describe physiological features and endocrinal factors, respectively.

Our studies on male and female Pai mice suggest that the chronic effects of t10c12-CLA on lean animals are dose-dependent and differ between sexes. Furthermore, the metabolic impact of t10c12-CLA involves various hormones and has system-wide effects on multiple metabolic pathways. Thus, interpreting the data from Pai mice requires careful consideration, and more work is needed to understand the mechanism of action of t10c12-CLA and its metabolic impact.

Abbreviations

489 BAT, brown adipose tissue; CPT1, carnitine palmitoyltransferase 1; CRP, C-reactive
490 protein; FA, fatty acids; FASN, fatty acid synthase; FGF21, fibroblast growth factor 21; IL-6,
491 interleukin-6; LA, linoleic acid; pai, *Propionibacterium acnes* isomerase; (p)AMPK,
492 phosphorylated AMP-activated protein kinase; PEG2, prostaglandin E2; (p)HSL,
493 phosphorylated hormone-sensitive lipase; t10c12-CLA, *trans* 10, *cis* 12-conjugated linoleic
494 acid; TC, total cholesterol; TGs, triglycerides; TNFα, tumour necrosis factor-alpha; UCP,
495 uncoupling protein; WAT, white adipose tissue; wt, wild-type;

496 **Ethics approval and consent to participate:**

497 All animal experiments followed the Committee for Experimental Animals of
498 Yangzhou University. All applicable institutional and/or national guidelines for the care and
499 use of animals were followed.

500 **Institutional Review Board Statement:**

501 The animal study protocol was approved by the Ethics Committee of Yangzhou
502 University (protocol code NSFC2020-SYXY-20 and dated 25 March 2020).

503 **Consent for publication:**

504 Not applicable

505 **Availability of data and materials:**

506 The datasets used and/or analysed during the current study are available from the
507 corresponding author upon reasonable request.

508 **Competing interests:**

509 The authors declare that they have no competing interests.

510 **Funding sources**

511 This work was supported by the National Key Research and Development Program
512 of China (2018YFC1003800), the Priority Academic Program Development of Jiangsu Higher
513 Education Institutions (PAPD), and the Jiangsu Funding Program for Excellent Postdoctoral
514 Talent.

515 **Acknowledgement**

We thank graduate students Qi Wang, Mei Liu, and Jiaqi Lu in our lab for their generous assistance in partial tests and Ms Yuyang Wang in our university for technique help in gas chromatography. We also thank Professor Hongjun Wang at the Medical University of South Carolina, USA, for the helpful discussion during the writing process and Ms Wenjing Gou's language assistance in preparing this manuscript.

Authors 'contributions:

Conceptualization, Y Rao and K Gou; Data curation, Y Rao, M Li, B Wang, Y Wang, and L Liang; Formal analysis, Y Rao and K Gou; Funding acquisition, Y Rao and K Gou; Investigation, Y Rao, M Li, B Wang, Y Wang and L Liang; Methodology, Y Rao, M Li, B Wang, Y Wang and L Liang; Project administration, K Gou; Software, Y Rao; Supervision, K Gou; Validation, K Gou; Visualization, Y Rao and L Liang; Writing – original draft, Y Rao; Writing – review & editing, K Gou. All authors proofread, made comments, and approved the report.

Supplementary data

This manuscript contains supplementary data.

References

1. Shen, W.; Baldwin, J.; Collins, B.; Hixson, L.; Lee, K.T.; Herberg, T.; Stames, J.; Cooney, P.; Chuang, C.C.; Hopkins, R., et al. Low level of trans-10, cis-12 conjugated linoleic acid decreases adiposity and increases browning independent of inflammatory signaling in overweight Sv129 mice. *Journal of Nutritional Biochemistry* **2015**, *26*, 616-625, doi:10.1016/j.jnutbio.2014.12.016.
2. den Hartigh, L.J.; Wang, S.R.; Goodspeed, L.; Wietecha, T.; Houston, B.; Omer, M.; Ogimoto, K.; Subramanian, S.; Gowda, G.A.N.; O'Brien, K.D., et al. Metabolically distinct weight loss by 10,12 CLA and caloric restriction highlight the importance of subcutaneous white adipose tissue for glucose homeostasis in mice. *Plos One* **2017**, *12*, doi:10.1371/journal.pone.0172912.
3. Rao, Y.; Li, S.L.; Li, M.J.; Wang, B.Z.; Wang, Y.Y.; Liang, L.W.; Yu, S.; Liu, Z.P.; Cui, S.; Gou, K.M. Transgenic mice producing the trans 10, cis 12-conjugated linoleic acid present reduced adiposity and increased thermogenesis and fibroblast growth factor 21 (FGF21). *J Nutr Biochem* **2023**, 10.1016/j.jnutbio.2023.109419, 109419, doi:10.1016/j.jnutbio.2023.109419.
4. Berkel, C.; Cacan, E. Trans-10, cis-12 conjugated linoleic acid- and caloric restriction-mediated upregulation of CNDP2 expression in white adipose tissue in rodents, with implications in feeding and obesity. *J Nutr Biochem* **2023**, *114*, 109269, doi:10.1016/j.jnutbio.2023.109269.
5. Wang, L.; Zhang, S.; Huang, Y.; You, W.; Zhou, Y.; Chen, W.; Sun, Y.; Yi, W.; Sun, H.; Xie, J., et al. CLA improves the lipo-nutritional quality of pork and regulates the gut microbiota in Heigai pigs. *Food Funct* **2022**, *13*, 12093-12104, doi:10.1039/d2fo02549c.

553 6. Kanter, J.E.; Goodspeed, L.; Wang, S.; Kramer, F.; Wietecha, T.; Gomes-Kjerulf, D.;
554 Subramanian, S.; O'Brien, K.D.; den Hartigh, L.J. 10,12 Conjugated Linoleic Acid-
555 Driven Weight Loss Is Protective against Atherosclerosis in Mice and Is Associated
556 with Alternative Macrophage Enrichment in Perivascular Adipose Tissue. *Nutrients*
557 **2018**, *10*, doi:10.3390/nu10101416.

558 7. Vaisar, T.; Wang, S.; Omer, M.; Irwin, A.D.; Storey, C.; Tang, C.; den Hartigh, L.J. 10,12-
559 Conjugated linoleic acid supplementation improves HDL composition and function
560 in mice. *J Lipid Res* **2022**, *63*, 100241, doi:10.1016/j.jlr.2022.100241.

561 8. Kim, J.H.; Kim, Y.; Kim, Y.J.; Park, Y. Conjugated linoleic acid: Potential health benefits
562 as a functional food ingredient. *Annu Rev Food Sci Technol* **2016**, *7*, 221-244,
563 doi:10.1146/annurev-food-041715-033028.

564 9. Marques, T.M.; Wall, R.; O'Sullivan, O.; Fitzgerald, G.F.; Shanahan, F.; Quigley, E.M.;
565 Cotter, P.D.; Cryan, J.F.; Dinan, T.G.; Ross, R.P., et al. Dietary trans-10, cis-12-
566 conjugated linoleic acid alters fatty acid metabolism and microbiota composition in
567 mice. *Br J Nutr* **2015**, *113*, 728-738, doi:10.1017/S0007114514004206.

568 10. Cuciniello, R.; Luongo, D.; Ferramosca, A.; Lunetti, P.; Rotondi-Aufiero, V.; Crispi, S.;
569 Zara, V.; Maurano, F.; Filosa, S.; Bergamo, P. Conjugated linoleic acid downregulates
570 Alzheimer's hallmarks in aluminum mouse model through an Nrf2-mediated
571 adaptive response and increases brain glucose transporter levels. *Free Radic Biol Med*
572 **2022**, *191*, 48-58, doi:10.1016/j.freeradbiomed.2022.08.027.

573 11. Cordoba-Chacon, J.; Sugasini, D.; Yalagala, P.C.R.; Tummala, A.; White, Z.C.; Nagao,
574 T.; Kineman, R.D.; Subbaiah, P.V. Tissue-dependent effects of cis-9,trans-11- and
575 trans-10,cis-12-CLA isomers on glucose and lipid metabolism in adult male mice. *J*
576 *Nutr Biochem* **2019**, *67*, 90-100, doi:10.1016/j.jnutbio.2019.01.020.

577 12. Clement, L.; Poirier, H.; Niot, I.; Bocher, V.; Guerre-Millo, M.; Krief, S.; Staels, B.;
578 Besnard, P. Dietary trans-10,cis-12 conjugated linoleic acid induces hyperinsulinemia
579 and fatty liver in the mouse. *J Lipid Res* **2002**, *43*, 1400-1409, doi:10.1194/jlr.m20008-
580 jlr200.

581 13. Kelley, D.S.; Bartolini, G.L.; Warren, J.M.; Simon, V.A.; Mackey, B.E.; Erickson, K.L.
582 Contrasting effects of t10,c12- and c9,t11-conjugated linoleic acid isomers on the fatty
583 acid profiles of mouse liver lipids. *Lipids* **2004**, *39*, 135-141, doi:10.1007/s11745-004-
584 1211-9.

585 14. Jaudszus, A.; Moeckel, P.; Hamelmann, E.; Jahreis, G. Trans-10,cis-12-CLA-caused
586 lipodystrophy is associated with profound changes of fatty acid profiles of liver, white
587 adipose tissue and erythrocytes in mice: possible link to tissue-specific alterations of
588 fatty acid desaturation. *Ann Nutr Metab* **2010**, *57*, 103-111, doi:10.1159/000319877.

589 15. Letona, A.Z.; Niot, I.; Laugerette, F.; Athias, A.; Monnot, M.C.; Portillo, M.P.; Besnard,
590 P.; Poirier, H. CLA-enriched diet containing t10,c12-CLA alters bile acid homeostasis
591 and increases the risk of cholelithiasis in mice. *J Nutr* **2011**, *141*, 1437-1444,
592 doi:10.3945/jn.110.136168.

593 16. Li, S.L.; Ma, S.Y.; Xu, B.R.; Fan, Z.Y.; Li, M.J.; Cao, W.G.; Gou, K.M. Effects of trans-10,
594 cis-12-conjugated linoleic acid on mice are influenced by the dietary fat content and
595 the degree of murine obesity. *Eur J Lipid Sci Tech* **2015**, *117*, 1908-1918,
596 doi:10.1002/ejlt.201400568.

597 17. Flippo, K.H.; Potthoff, M.J. Metabolic Messengers: FGF21. *Nat Metab* **2021**, *3*, 309-317,
598 doi:10.1038/s42255-021-00354-2.

599 18. Subbaiah, P.V.; Gould, I.G.; Lal, S.; Aizezi, B. Incorporation profiles of conjugated
600 linoleic acid isomers in cell membranes and their positional distribution in
601 phospholipids. *Biochim Biophys Acta* **2011**, *1811*, 17-24,
602 doi:10.1016/j.bbalip.2010.09.004.

603 19. Furuyashiki, T.; Narumiya, S. Stress responses: the contribution of prostaglandin E(2)
604 and its receptors. *Nat Rev Endocrinol* **2011**, *7*, 163-175, doi:10.1038/nrendo.2010.194.

605 20. Zeigerer, A.; Sekar, R.; Kleinert, M.; Nason, S.; Habegger, K.M.; Muller, T.D.
606 Glucagon's metabolic action in health and disease. *Compr Physiol* **2021**, *11*, 1759-1783,
607 doi:10.1002/cphy.c200013.

608 21. Saper, C.B.; Lowell, B.B. The hypothalamus. *Curr Biol* **2014**, *24*, R1111-1116,
609 doi:10.1016/j.cub.2014.10.023.

610 22. Cypess, A.M.; Weiner, L.S.; Roberts-Toler, C.; Franquet Elia, E.; Kessler, S.H.; Kahn,
611 P.A.; English, J.; Chatman, K.; Trauger, S.A.; Doria, A., et al. Activation of human
612 brown adipose tissue by a beta3-adrenergic receptor agonist. *Cell Metab* **2015**, *21*, 33-
613 38, doi:10.1016/j.cmet.2014.12.009.

614 23. Contreras, C.; Gonzalez-Garcia, I.; Seoane-Collazo, P.; Martinez-Sanchez, N.; Linares-
615 Pose, L.; Rial-Pensado, E.; Ferno, J.; Tena-Sempere, M.; Casals, N.; Dieguez, C., et al.
616 Reduction of hypothalamic endoplasmic reticulum stress activates browning of white
617 fat and ameliorates obesity. *Diabetes* **2017**, *66*, 87-99, doi:10.2337/db15-1547.

618 24. Contreras, C.; Fondevila, M.F.; Lopez, M. Hypothalamic GRP78, a new target against
619 obesity? *Adipocyte* **2018**, *7*, 63-66, doi:10.1080/21623945.2017.1405878.

620 25. Martins, L.; Seoane-Collazo, P.; Contreras, C.; Gonzalez-Garcia, I.; Martinez-Sanchez,
621 N.; Gonzalez, F.; Zalvide, J.; Gallego, R.; Dieguez, C.; Nogueiras, R., et al. A functional
622 link between ampk and orexin mediates the effect of bmp8b on energy balance. *Cell*
623 *Rep* **2016**, *16*, 2231-2242, doi:10.1016/j.celrep.2016.07.045.

624 26. Chemelli, R.M.; Willie, J.T.; Sinton, C.M.; Elmquist, J.K.; Scammell, T.; Lee, C.;
625 Richardson, J.A.; Williams, S.C.; Xiong, Y.M.; Kisanuki, Y., et al. Narcolepsy in orexin
626 knockout mice: Molecular genetics of sleep regulation. *Cell* **1999**, *98*, 437-451, doi:Doi
627 10.1016/S0092-8674(00)81973-X.

628 27. Ashwell, M.S.; Ceddia, R.P.; House, R.L.; Cassady, J.P.; Eisen, E.J.; Eling, T.E.; Collins,
629 J.B.; Grissom, S.F.; Odle, J. Trans-10, cis-12-conjugated linoleic acid alters hepatic gene
630 expression in a polygenic obese line of mice displaying hepatic lipidosis. *J Nutr*
631 *Biochem* **2010**, *21*, 848-855, doi:10.1016/j.jnutbio.2009.06.013.

632 28. Vyas, D.; Kadegowda, A.K.; Erdman, R.A. Dietary conjugated linoleic acid and
633 hepatic steatosis: species-specific effects on liver and adipose lipid metabolism and
634 gene expression. *J Nutr Metab* **2012**, *2012*, 932928, doi:10.1155/2012/932928.

635 29. Laryea, G.; Schutz, G.; Muglia, L.J. Disrupting hypothalamic glucocorticoid receptors
636 causes HPA axis hyperactivity and excess adiposity. *Mol Endocrinol* **2013**, *27*, 1655-
637 1665, doi:10.1210/me.2013-1187.

638 30. Nicolaides, N.C.; Charmandari, E.; Kino, T.; Chrousos, G.P. Stress-related and
639 circadian secretion and target tissue actions of glucocorticoids: Impact on health. *Front*
640 *Endocrinol (Lausanne)* **2017**, *8*, 70, doi:10.3389/fendo.2017.00070.

641 31. Krilov, L.; Nguyen, A.; Miyazaki, T.; Unson, C.G.; Bouscarel, B. Glucagon receptor
642 recycling: role of carboxyl terminus, beta-arrestins, and cytoskeleton. *Am J Physiol-Cell*
643 *Ph* **2008**, *295*, C1230-C1237, doi:10.1152/ajpcell.00240.2008.

644 32. Charbonneau, A.; Unson, C.G.; Lavoie, J.M. High-fat diet-induced hepatic steatosis
645 reduces glucagon receptor content in rat hepatocytes: potential interaction with acute
646 exercise. *J Physiol-London* **2007**, *579*, 255-267, doi:10.1113/jphysiol.2006.121954.

647 33. Sammons, M.F.; Lee, E.C.Y. Recent progress in the development of small-molecule
648 glucagon receptor antagonists. *Bioorg Med Chem Lett* **2015**, *25*, 4057-4064,
649 doi:10.1016/j.bmcl.2015.07.092.

650 34. Perry, R.J.; Zhang, D.; Guerra, M.T.; Brill, A.L.; Goedeke, L.; Nasiri, A.R.; Rabin-Court,
651 A.; Wang, Y.; Peng, L.; Dufour, S., et al. Glucagon stimulates gluconeogenesis by
652 INSP3R1-mediated hepatic lipolysis. *Nature* **2020**, *579*, 279-283, doi:10.1038/s41586-
653 020-2074-6.

654 35. Hayashi, Y. Glucagon regulates lipolysis and fatty acid oxidation through inositol
655 triphosphate receptor 1 in the liver. *J Diabetes Investig* **2021**, *12*, 32-34,
656 doi:10.1111/jdi.13315.

657 36. Kleinert, M.; Sachs, S.; Habegger, K.M.; Hofmann, S.M.; Muller, T.D. Glucagon
658 regulation of energy expenditure. *Int J Mol Sci* **2019**, *20*, doi:10.3390/ijms20215407.

659 37. Schlein, C.; Talukdar, S.; Heine, M.; Fischer, A.W.; Krott, L.M.; Nilsson, S.K.; Brenner,
660 M.B.; Heeren, J.; Scheja, L. Fgf21 lowers plasma triglycerides by accelerating
661 lipoprotein catabolism in white and brown adipose tissues. *Cell Metab* **2016**, *23*, 441-
662 453, doi:10.1016/j.cmet.2016.01.006.

663 38. Bookout, A.L.; de Groot, M.H.; Owen, B.M.; Lee, S.; Gautron, L.; Lawrence, H.L.; Ding,
664 X.; Elmquist, J.K.; Takahashi, J.S.; Mangelsdorf, D.J., et al. FGF21 regulates metabolism
665 and circadian behavior by acting on the nervous system. *Nat Med* **2013**, *19*, 1147-1152,
666 doi:10.1038/nm.3249.

667 39. Holland, W.L.; Adams, A.C.; Brozinick, J.T.; Bui, H.H.; Miyauchi, Y.; Kusminski, C.M.;
668 Bauer, S.M.; Wade, M.; Singhal, E.; Cheng, C.C., et al. An FGF21-adiponectin-ceramide
669 axis controls energy expenditure and insulin action in mice. *Cell Metab* **2013**, *17*, 790-
670 797, doi:10.1016/j.cmet.2013.03.019.

671 40. Henriksen, E.J.; Teachey, M.K.; Taylor, Z.C.; Jacob, S.; Ptock, A.; Kramer, K.;
672 Hasselwander, O. Isomer-specific actions of conjugated linoleic acid on muscle
673 glucose transport in the obese Zucker rat. *Am J Physiol Endocrinol Metab* **2003**, *285*, E98-
674 E105, doi:10.1152/ajpendo.00013.2003.

675 41. Tsuboyama-Kasaoka, N.; Takahashi, M.; Tanemura, K.; Kim, H.J.; Tange, T.;
676 Okuyama, H.; Kasai, M.; Ikemoto, S.; Ezaki, O. Conjugated linoleic acid
677 supplementation reduces adipose tissue by apoptosis and develops lipodystrophy in
678 mice. *Diabetes* **2000**, *49*, 1534-1542, doi:10.2337/diabetes.49.9.1534.

679